

## Monitoring transfer of spins

DOI: 10.1002/anie.200123456

## Spin Coherence Transfer in Chemical Transformations Monitored by NMR\*\*

M. Sabieh Anwar, Christian Hilty, Chester Chu,  
Kimberly L. Pierce and Alex Pines\*

**We demonstrate the use of micro-scale nuclear magnetic resonance (NMR) for studying the transfer of spin coherence in non-equilibrium chemical processes, using spatially separated NMR encoding and detection coils. As an example, we provide the map of chemical shift correlations for the amino acid alanine as it transitions from the zwitterionic to the anionic form. Our method is unique in the sense that it allows us to track the chemical migration of encoded nuclear spins during the course of chemical transformations.**

There exists an astounding diversity of chemical transformations such as chemical reactions, protein folding and unfolding, cell division and disease progression. The chemist's role is to monitor these changes. For this purpose, analytical chemistry provides us with a mélange of techniques. The transformation usually manifests itself in a change of some observable property and the choice of the method of monitoring these changes depends on the technique's sensitivity, time resolution and the ability to distinguish between the unmodified and modified states. For example, HPLC has been used to follow the oxidation of glucose;<sup>[1]</sup> FTIR has been used for monitoring yields of microwave assisted fast organic reactions<sup>[2]</sup> as well as the hydrolysis of monochloroacetate;<sup>[3]</sup> enzyme reactions in microreactors have been characterized by fluorescence imaging<sup>[4]</sup> and gas chromatography has been employed to determine the progress of Swern oxidations of alcohols.<sup>[5]</sup>

Included in this list is NMR: a rich spectroscopic technique known for providing unparalleled chemical information at the molecular level. Not surprisingly, it is routinely used for monitoring chemical reactions and conformational changes. Recently, NMR has also been used in micro-flow systems<sup>[6]</sup> for studying the kinetics of chemical reactions,<sup>[7]</sup> protein unfolding dynamics<sup>[8]</sup> and flow profiles.<sup>[9]</sup> These NMR techniques directly couple to "lab-on-a-chip"

devices, multiplexed micro-total analysis systems ( $\mu$ -TAS) and systems for on-line monitoring of biological and pharmaceutical assays.<sup>[10]</sup> Some particular advantages of flow based miniaturized NMR include: small volumes of reagents, especially useful when the reagents are expensive or hazardous; increased mass sensitivities;<sup>[11]</sup> the possibility of hyphenation with complementary spectroscopy and separation techniques;<sup>[12]</sup> high-throughput, multiplexed detection;<sup>[13]</sup> and attaining high-purities and yields.<sup>[14]</sup> Specialized microreactors can also be used to enhance the efficiency of mixing, increasing rates of reaction and optimizing reaction pathways or isolating intermediates by modulation of coil residence times.<sup>[5,15]</sup>

Previous NMR studies have followed the progress of chemical changes by monitoring the concentrations of molecules as a function of time. This is tantamount to detecting NMR spectra before and after the chemical reaction and monitoring the difference between the two. For example, Ciobanu et al. investigated the xylose-borate complexation reaction by measuring the build up of product peaks with time<sup>[7a]</sup> and Wensink et al. monitored the benzaldehyde-aniline reaction by measuring the time-dependent peak areas in the reactant and product spectra.<sup>[7b]</sup> The experimental method proposed in this paper is different from the aforementioned experiments because it monitors spin coherence *transfers* between the reactant and the product, rather than measuring coherence *amplitudes* in the product. Thus, apart from kinetic data, it can also provide mechanistic information.

The measurement of coherence transfer is achieved by using two separate coils for encoding and detection of NMR coherence, following a method termed remote detection.<sup>[9,16]</sup> Previously, the two coil approach has been used for the independent optimization of the encoding and detection steps, or for measuring flow dispersion.<sup>[9]</sup> Tracking spin coherence transfers in chemical processes is a new application of the remote detection methodology.

Consider the chemical transformation in which **A** converts to **C** in the presence of **B** which can either be another reactant or a medium inducing the chemical transformation. The nuclear spins in **A** change their chemical environment as the chemical transformation takes place. The altered environment results in a change in chemical shift which can be detected by NMR. If the **A** spins have been encoded *prior* to mixing with **B**, it is possible for the two-coil NMR experiment to connect the spins in **C** with those in **A**. The results can be presented in the form of a correlation map (discussed below). This allows us to track the transfer of coherences *during* the chemical transformation and can be a valuable method for a) distinguishing between different reaction mechanisms and b) sensing the presence of the reagent **B** and therefore acting as a probe for chemical environments.

As a model system, we consider the deprotonation of the amino acid alanine in the presence of a basic medium.<sup>[18]</sup> At pH=7, the molecule exists as the zwitterion  $\text{NH}_3^+ \text{CH}(\text{CH}_3) \text{COO}^-$  and at basic pH (e.g., 14), the amide group is deprotonated resulting in the anion  $\text{NH}_2 \text{CH}(\text{CH}_3) \text{COO}^-$ , the  $\text{pK}_a$  value for the amide proton being 9.7. The increased negative charge on the amide group results in a higher negative charge on the electron-withdrawing groups, increasing the chemical shielding effect and resulting in an upfield shift of the proton resonances. For example, The CH and  $\text{CH}_3$  ( $\alpha$  and  $\beta$ ) protons shift upfield by about 0.6 and 0.4 ppm. With our spatially and temporally separated encoding and detection steps, we map the coherence transfers in the  $\alpha$  and  $\beta$  protons as the environment switches from neutral to basic mediums. For the proof of principle experiment, we used 2.0M alanine in  $\text{D}_2\text{O}$  (pD=7.0) as the liquid **A** and 10.0M NaOD in  $\text{D}_2\text{O}$  (pD=14.0) as the basic medium **B**.

[\*] Dr. M. S. Anwar, Dr. C. Hilty, C. Chu, Dr. K. L. Pierce, Prof Alex Pines  
Department of Materials Science  
Lawrence Berkeley National Lab  
1 Cyclotron Road, Bldg. 11-D64, Berkeley, CA 94720, US  
Fax: (+1) 510-486-5744  
E-mail: [sabieh@berkeley.edu](mailto:sabieh@berkeley.edu)

[\*\*] This work was supported by the Director, Office of Science, Office of Basic Energy Sciences, Materials Sciences and Engineering Division, of the U.S. Department of Energy under Contract No. DE-AC03-76SF00098. C.H. acknowledges support from the Schweizerischer Nationalfonds through a post-doctoral fellowship. The authors thank Erin E. McDonnell for hardware assistance and L. Bouchard for useful discussions.

Supporting information for this article is available on the WWW under <http://www.angewandte.org> or from the author.

Figure 1a shows the schematic setup of our experiment. The liquids **A** and **B** are syringe injected into micro-capillaries **1** and **2**. The radio-frequency (RF) coil **E** encodes chemical shift information into proton spins in **A**, the liquids are then allowed to mix in a micro-tee mixer **T**. Mixing continues as the streams of liquids jointly flow through the outlet capillary **3** where they are finally detected with the RF micro-coil **D**. The encoding and detection is carried out in the homogeneous region of a high field NMR magnet.

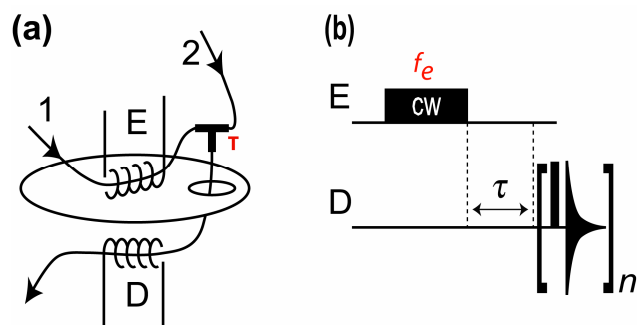


**Figure 1.** (a) Schematics of the experimental NMR setup and (b) pulse sequence used for monitoring the spin coherence transfer. The encoding and detection coils are represented as **E** and **D**, the inlet capillaries are **1** and **2** and mixing takes place inside and after the mixer **T**. In b, the transmitter frequency in the encoding coil is  $f_e$ ,  $\tau$  is a fixed delay and detection comprises a train of  $n$   $90^\circ$  hard pulses followed by acquisition.

The encoded spins travel from **E** to **D** in a certain length of time, called the time of flight  $t_f$ , which depends on the flow rate. Figure 1(b) shows the NMR pulse sequence for measuring  $t_f$  and also for the remote detection of the magnetization. The sequence comprises a long (500 ms) pulse of low power continuous wave (CW) irradiation on **E**. The frequency of the encoding pulse  $f_e$  can be adjusted so that only one narrow spectral region is excited and, in the process, saturated. After a time allowing for physical travel of the encoded species, the detection is made in **D** with  $90^\circ$  pulses and acquisition periods of length  $t_{acq}$ . The pulse—detect combination is repeated  $n$  times, to obtain signal from all encoded spins.

Alternatively, it is also possible to use high power, short duration  $90^\circ$  pulses for the encoding<sup>[16]</sup>. However, we encode more spins by using longer duration low power RF, as this irradiates several coil volumes of the flowing liquid. In principle, this approach is equivalent to using a bigger sized encoding coil.

The injected spins start off in the equilibrium magnetization  $I_z$ . A  $90^\circ$  pulse in **D** will convert these spins into observable  $I_x$ , but if the spins have been previously encoded (saturated) in **E**, the pulse in **D** leaves them in an unobservable depolarized state. As a result, unencoded spins will produce the maximum intensity in the detection coil spectra, and the intensity will be reduced for the encoded spins. The resulting time of travel curves for two flow rates are shown in Figure 2. The point of minimum intensity in these curves corresponds to the modal time of flight  $t_f$  between the two coils. It can be seen that the breadth of the dip is bigger for the slower flow rate and is indicative of axial dispersion of the fluid as a consequence of laminar flow. The dispersion of the spins compromises the sensitivity of a single acquisition in the detection coil, but can be compensated to an extent by summing over the FID's obtained from a selection of points around  $t_f$ . These points are represented by the colored regions in the travel curves.

The experiment that measures the transfer of spin coherence in a chemical process uses the same pulse sequence as given in Figure 2(b). The parameters  $\tau$  and  $n$  are selected based on the time of travel curve, so that the acquisition extends over the dip (shown as the colored regions in Figure 2). In reminiscence of absorption mode continuous wave NMR spectroscopy, the encoding frequency  $f_e$  is

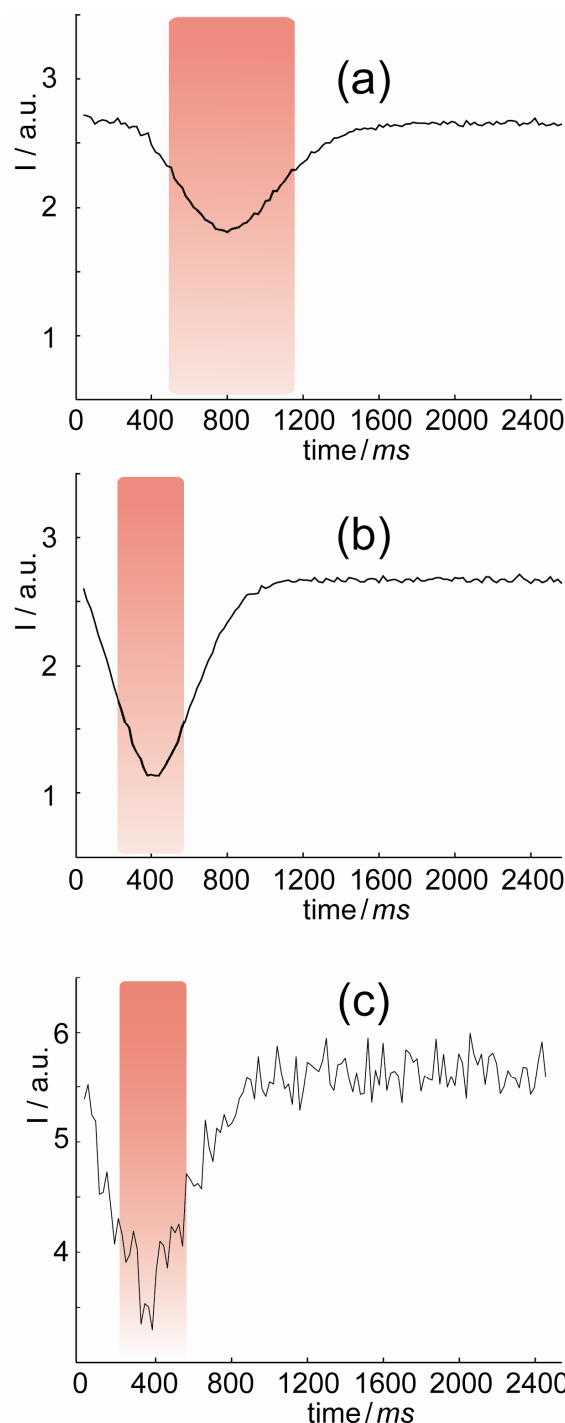


**Figure 2.** Time of travel curves for the  $\text{CH}_3$  peak in ethanol for flow rates of (a)  $25 \mu\text{L min}^{-1}$ , (b)  $50 \mu\text{L min}^{-1}$  and (c) curve for the  $\beta$  protons of alanine flowing at  $50 \mu\text{L min}^{-1}$ . The delay  $\tau \approx 0$  ms and  $n = 128$  detection pulses are applied in **D** with  $t_{acq} = 20$  ms. The curve in (c) is an average over 32 scans. For the data shown,  $t_f$  is (a) 840, (b) 420 and (c) 380 ms.

swept across the range of frequencies in the encoding coil, saturating the individual peaks one by one and if an encoded peak changes its chemical environment during mixing, its chemical shift will appear shifted in the detection coil. It is thus possible to map out correlations between chemical shifts in the encoded and detected dimensions.

The correlation maps for unmixed ethanol (control experiment) and the zwitterionic and anionic forms of alanine are shown in Figure 3. For the ethanol experiment, the spectra do not change across the encoding and detection dimensions as there is no change in chemical environment between **E** and **D**, so the alcohol peaks appear in the two-dimensional correlation map along a diagonal, which is shown by a blue line in the Figure. For the alanine, the  $\alpha$  and  $\beta$  protons shift upfield by 0.6 and 0.4 ppm. These shifts are indicated by the presence of off-diagonal peaks in Figure 4b, which correlate the state *before* and *after* the introduction of the basic NaOD solution. Note that the frequency axes for the encoding and detection coils are arbitrarily calibrated, and appear shifted with respect to each other. This is a result of applying a small magnetic field gradient along the vertical axis to avoid effects from residual cross-talk between the two coils. In the correlation spectra shown here, it is possible to determine the location of the diagonal from a reactant/product peak that does not change in chemical shift. In more complex cases, it may be desirable to add a small amount of a reference compound, such as TMS, to the sample for this purpose.

This approach of correlating the pre-mixed and post-mixed spectra enables us to directly track the coherence of a spin as it changes its chemical shift due to changes in chemical environment.

Rapid mixing is crucial for the experiment. In the present case, diffusional mixing in a 100  $\mu\text{m}$  wide channel was used. This mechanism was sufficient for the present application that relied on the exchange of protons, which have a high diffusivity, and will also be adequate for a number of other solutes. In case of reactants with large molecular weight, or solutions of high viscosity, it may be desirable to use more advanced microfluidic mixing technologies.<sup>[19]</sup>

The method presented here is applicable to any chemical transformation that takes place within the spin-lattice relaxation time of the reactants. This relaxation time is on the order of seconds when observing protons, and on the order of tens of seconds when observing carbon.

Chemical changes that can be characterized by the presented method include, but are by no means limited to: changes in the degree of protonation or deprotonation, solvation and complexation,<sup>[20]</sup> folding and unfolding of proteins<sup>[21]</sup> and changes in chemical shift induced by chemical reactions. All of these changes will appear as off-diagonal peaks in the *e-d* correlation map, and their presence can be used as a sensitive probe for detecting changes in chemical environments of the spins.

In future experiments, we are considering improvements to our experimental setup by increasing the degree of mixing between the incoming liquids, improving the spectral resolution by susceptibility matching of the microcoils<sup>[21b]</sup> and the possibility of using stopped-flow<sup>[22]</sup> for higher sensitivity. We are looking into the possibility of investigating more complicated chemical reactions and modifying our pulse sequences for tracking changes in J couplings. With the time of flight degree of freedom, it is also possible to follow the kinetics of chemical reactions in addition to their mechanisms. Our method also shows promise for detecting multiple parallel or sequential chemical reactions in more complex microfluidic devices in a single experiment. Thereby, a pulsed field gradient can be used to spatially encode spectra from different inlet streams, which are detected after convergence in the detection coil. This strategy could for example be used to enable multiplexed combinatorial screening of pharmaceutical and biochemical compounds.<sup>[23]</sup>

## Experimental Section

All experiments were performed on a Bruker Avance spectrometer with a proton Larmor frequency of 300 MHz. The PEEK capillaries (Upchurch Scientific) have internal diameters 100  $\mu\text{m}$  (**1** and **3**) and 150  $\mu\text{m}$  (**2**) and a consistent outer diameter of 360  $\mu\text{m}$ , which fits into the micro-tee mixer (Upchurch Scientific) with an internal swept volume of 0.95  $\mu\text{L}$ . The fluid was delivered to the NMR magnet through 1/16 inch O.D. diameter Teflon tubes. The coils **E** and **D** are solenoidal micro-coils, both of them hand-wound and each being 3 mm in length. This translates to a detection volume of about 20 nL. All chemicals used were obtained from a commercial supplier (Sigma Aldrich). The liquids were injected with a syringe pump (Harvard Apparatus PHD 22/2000 HP) and flow rates typically used varied between 25 and 100  $\mu\text{L min}^{-1}$ . Prior to all experiments, the microcapillaries were purged with acetone and then air to remove any background signal. The 90° high power pulse widths were 1.1 and 1  $\mu\text{s}$  for the encoding and detection coils. The encoding comprised a long pulse (500 ms) of CW irradiation. For the remote correlation experiment, the frequency was swept over a range of 10.6 ppm in steps of 0.33 ppm. The CW encoding power level used was 25 Hz compared to a power of 250 KHz used for the hard pulse.

**Keywords:** nuclear magnetic resonance · spin chemistry · reaction mechanisms · microfluidic flow · NMR titration

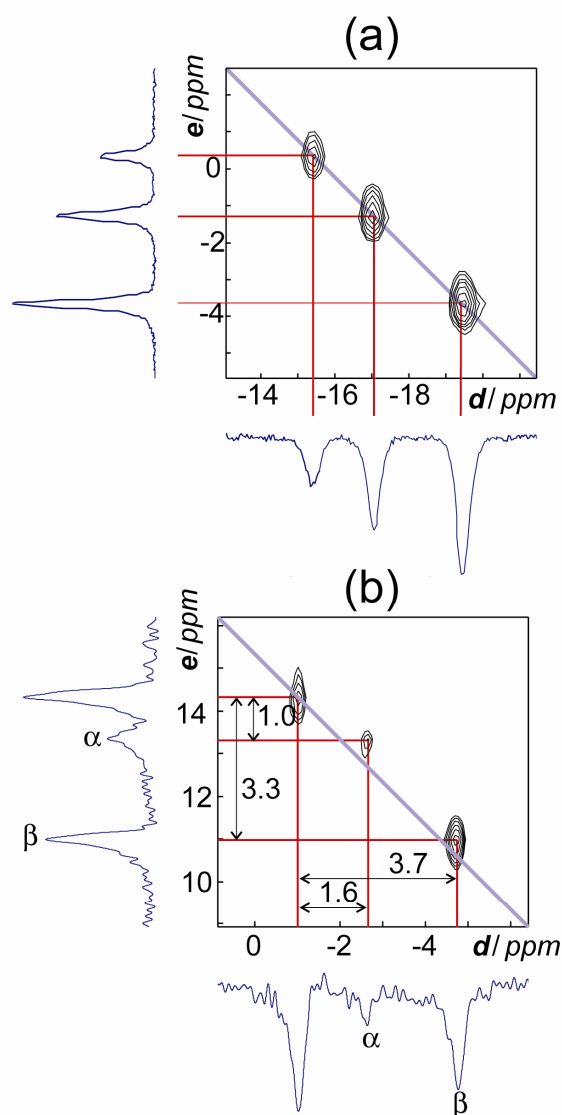


**Figure 3.** (a) The correlation map for unmixed ethanol and (b) the correlation map between the  $\alpha$  and  $\beta$  protons in the zwitterionic and the anionic forms of alanine. The axes  $d$  and  $e$  are chemical shift axes on the detection and encoding coils with units in ppm (uncalibrated). For comparison, the directly detected spectra, using the respective coils, are superposed on the axes. Intensity from unencoded spins is removed by subtraction of the respective baseline in each experiment. The map in (a) was obtained using a flow rate of  $25 \mu\text{L min}^{-1}$ , and an encoding frequency step size of 100 Hz whereas (b) was acquired with a flow rate of  $50 \mu\text{L min}^{-1}$ , and an encoding frequency step size of 100 Hz. The unlabelled peak in (b) is assigned to the residual proton signal in the  $\text{NaOD}/\text{D}_2\text{O}$ .

Received: ((will be filled in by the editorial staff))  
Published online on ((will be filled in by the editorial staff))

- [1] C. Basheer, S. Swaminathan, H.K. Lee, S. Valiyaveetil, *ChemCommun.* **2005**, 409–410.
- [2] J. Yoshida, *ChemCommun.* **2005**, 4509–4516.
- [3] N. Kaun, S. Kulka, J. Frank, U. Schade, M.J. Vellekoop, M. Harasek, B. Lendl, *Analyst* **2006**, *131*, 489–494.
- [4] G.H. Seong, R.M. Crooks, *J. Am. Chem. Soc.* **2002**, *124*, 13360–13361.
- [5] T. Kawaguchi, H. Miyata, K. Ataka, K. Mae, J. Yoshida, *Angew. Chem. Int. Ed.* **2005**, *44*, 2413–2416.
- [6] D.L. Olson, T.L. Peck, A.G. Webb, R.L. Magin, J.V. Sweedler, *Science* **1995**, *270*, 1967; b) A.M. Wolters, D.A. Jayawickrama, J.V. Sweedler, *Curr. Opinion Chem. Bio.*, **2002**, *6*, 711–716.
- [7] a) L. Ciobanu, D.A. Tayawickrama, X. Zhang, A.G. Webb, J.V. Sweedler, *Angew. Chem. Int. Ed.* **2003**, *42*, 4669–4672; b) A. Wensink, F. Benito-Lopez, D.C. Hermes, W. Verboom, H.J.G.E. Gardeniers, D.N. Reinhoudt, A.V.D. Berg, *Lab Chip* **2005**, *5*, 280–284.
- [8] M. Kakuta, D.A. Jayawickrama, A.M. Wolters, A. Manz, J.V. Sweedler, *Anal. Chem.* **2002**, *74*, 4191.
- [9] C. Hilty, E.E. McDonnell, J. Granwehr, K.L. Pierce, S.I. Han, A. Pines, *PNAS* **2003**, *102*, 14960–14963
- [10] J. Clayton, *Nature Methods* **2005**, *2*, 621.
- [11] D.A. Seeber, R.L. Cooper, L. Ciobanu, C.H. Pennington, *Rev. Sci. Instrum.* **2001**, *72*, 2171.
- [12] D.A. Jayawickrama, J.V. Sweedler, *Anal. Chem.* **2004**, *76*, 4894–4900.
- [13] a) D. Raftery, *Anal. Bioanal. Chem.* **2004**, *378*, 1403–1404; b) T. Hou, J. Smith, E. MacNamara, M. Macnaughtan, D. Raftery, *Anal. Chem.*, **2001**, *73*, 2541–2546.
- [14] P. Watts, S.J. Haswell, *Chem. Soc. Rev.* **2005**, *34*, 235–246.
- [15] a) W. Ehrfeld, V. Hessel, H. Lowe, *Microreactors: New technology for modern chemistry*, Wiley-VCH, New York, 2000; b) S.J. Haswell, R.J. Middleton, B. O'Sullivan, V. Skelton, P. Watts, P. Styring, *Chem. Commun.* **2001**, 391–398.
- [16] a) A.J. Moulé, M.M. Spence, S.I. Han, J.A. Seeley, K.L. Pierce, S. Suxena, A. Pines, *PNAS* **2003**, *100*, 9122–9127.
- [17] a) J. Granwehr, E. Harel, S.I. Han, S. Garcia, A. Pines, P.N. Sen, Y.Q. Song, *Phys. Rev. Lett.* **2005**, *95*, 075503; b) C. Hilty, E.E. McDonnell, J. Granwehr, K.L. Pierce, S.I. Han, A. Pines, *PNAS* **2003**, *102*, 14960–14963
- [18] a) Jones M, *Organic Chemistry*, W.W. Norton & Co., 1997, p. 1348; b) J.L. Yarger, R. A. Nieman, A.L. Bieber, *J. Chem. Edu.* **1997**, *74*, 243–246.
- [19] a) P.K. Yuen, G. Li, Y. Bao, U.R. Müller, *Lab Chip* **2003**, *3*, 46; b) L.E. Locascio, *Anal. Bioanal. Chem.* **2004**, *379*, 325–327; c) R.S. Macomber, *J. Chem. Ed.* **1992**, *69*, 375–378.
- [20] R.P. Sijbesma, A.P.M. Kentgens, R.J.M. Nolte, *J. Org. Chem.* **1991**, *56*, 3199–3201.
- [21] a) M.C.R. Shastry, H. Roder, *Nature Struct. Biol.* **1998**, *5*, 385–392. b) M. Kakuta, D.A. Jayawickrama, A.M. Wolters, A. Manz, J.V. Sweedler, *Anal. Chem.* **2003**, *75*, 956–960.
- [22] a) A. Gomez-Hens, D. Perez-Bendito, *Analytica Chim. Acta* **1991**, *242*, 147–177; b) D.L. Olson, M.E. Lacey, A.G. Webb, J.V. Sweedler, *Anal. Chem.* **1999**, *71*, 3070–3076.



## Monitoring transfer of spins

*M. S. Anwar, C. Hilty, C. Chu, K. L. Pierce, A. Pines\**

### Spin coherence transfer in chemical processes monitored by NMR

The use of micro-scale nuclear magnetic resonance (NMR) for studying the transfer of spin coherence in non-equilibrium chemical processes, using spatially separated NMR encoding and detection coils is demonstrated. As an example, we provide the map of chemical shift correlations for the amino acid alanine as it transitions from the zwitterionic to the anionic form. Our method is unique in the sense that it allows us to track the chemical migration of encoded nuclear spins during the course of chemical transformations.

